

Prediction of the Vickers hardness in austempered ductile irons using neural networks

M. A. Yescas*

University of Cambridge, Department of Materials Science and Metallurgy, Pembroke Street, Cambridge CB2 3QZ, U.K.

To the design engineer, hardness often means an easily measured quantity which indicates something about the strength and heat treatment of a metal. Austempered ductile iron (ADI) is an alloyed and heat treated ductile cast iron which has a good combination of mechanical properties. This paper describes a neural network model created with a Bayesian framework using published data. The model created is capable of successfully expressing the hardness of austempered ductile irons and can be used as a tool in the processing or design of ADI. The computer programs associated with the work have been made freely available at: <http://www.msm.cam.ac.uk/map/mapmain.html>

Keywords: hardness, austempering, bainite, ductile iron, retained austenite, neural networks

Introduction

Austempered ductile cast irons have complex microstructures consisting of a mixture of bainitic ferrite, retained austenite, untempered martensite and carbides. It is not easy to characterise the microstructure on a routine basis, but it is known that the details of the microstructure to a large extent determine the mechanical properties of the iron.¹

Hardness, on the other hand, is easily measured and widely reported. It is frequently used as a quality control parameter to ensure that the process and materials used are behaving in a reproducible manner.

Since the hardness correlates with the microstructure, it can also be used to optimise the production process. For example, it is known that during austempering, the microstructure is very sensitive to the time it is held at the isothermal transformation temperature.² Thus, a short time leads to a final microstructure which is predominantly martensitic and very hard. As the transformation time is increased, the formation of bainitic ferrite and the consequent carbon enrichment of the residual austenite leads to a softer microstructure. Prolonged austempering causes the decomposition of austenite into carbides and ferrite, which leads to a small increase in hardness. The precipitation of carbides is detrimental to properties, so the hardness can be used as a simple way of optimising the austempering time in the development process.

The problem of designing these austempered ductile irons clearly involves many variables and great complexity.³ The purpose of the work presented here is to develop a model capable of predicting the hardness of ADI, as a function of the main variables affecting hardness using a neural network technique within a Bayesian framework.⁴

The technique

A neural network is a general method of regression analysis in which a flexible non-linear function is fitted to experimental data, the details of which have been reviewed extensively.⁴⁻⁶ It is nevertheless worth emphasising some of the features of the particular method used here, which is attributable to MacKay.^{7,8} The method, in addition to providing an indication of the perceived level of noise in the output, gives error bars representing the uncertainty in the fitting parameters. The method recognises that there are many functions which can be fitted or extrapolated into uncertain regions of the input space, without excessively compromising the fit in adjacent regions which are rich in accurate data. Instead of calculating a unique set of weights, a probability distribution of sets of weights is used to define the fitting uncertainty. The error bars therefore become large when data are sparse or locally noisy.

The Bayesian framework for neural networks has a further advantage. The significance of the input variables is automatically quantified.^{7,8} Consequently the significance, perceived by the model of each input variable can be compared against metallurgical experience.

The general form of the model is as follows, with y representing the output variable and x_j the set of inputs.

$$y = \sum_i w_{ij}^{(2)} h_i + \theta^{(2)} \quad (1)$$

$$\text{where } h_i = \tanh \left(\sum_j w_{ij}^{(1)} x_j + \theta_i^{(1)} \right)$$

The subscript i represents the hidden units (Fig. 1), the θ terms are biases and w_{ij} the weights. Thus, the statement of Eq. 1 together with the weights and coefficients defines the function giving the output as a function of the inputs.

A potential difficulty with the use of powerful regression methods is the possibility of overfitting data. One procedure to avoid this is that the experimental data are divided into two sets, a *training* data set and a *test* data set. The model is produced using only the training data. The test data are then used to check that the model behaves

* Author for correspondence
e-mail: Miguel.Yescas@corusgroup.com

correctly when presented with previously unseen data. The training process involves a search for the optimum non-linear relationship between the input and the output data and is computer intensive. Once the network is trained, estimation of the outputs for any given set of inputs is very fast. The details of the ways in which overfitting is controlled are described in ^{7,8}

The variables

Analysis is based on published data. Fortunately, hardness is a value which is easily measured and hence is frequently reported. Hardness is strictly a function of the microstructure and solid solution strengthening. Both of the latter depend on chemical composition and heat treatment. Therefore, the inputs to the model included the detailed chemical composition in wt.%, the austenitising temperature in °C and time in minutes (T_γ and t_γ respectively), and the austempering temperature and time (T_A and t_A respectively), Table 1. This is almost all that is necessary to define hardness. Chromium and vanadium were not included since these elements are not common alloying elements in ADI, and indeed, there are few data available. A total of 1822 experimental data were collected from the published literature⁹⁻⁷³ and digitised; elementary checks on the data included an assessment of the minimum and maximum values for each variable.

As has been shown previously,³ the austempering time is better expressed in logarithmic form as $\log\{t_A\}$ rather than t_A . However, it is conceivable that there might be some unknown process which varies directly with t_A so both the logarithmic time and the time were included as input variables. This has the advantage of avoiding bias in the inputs; the method used here has automatic relevance determination⁴ and hence sets the weights associated with an irrelevant input to small or zero values should that be justified.

It is emphasised that unlike linear regression analysis, the ranges stated in Table 1 cannot be used to define the range of applicability of the neural network model. This is because the inputs are in general expected to interact. It is

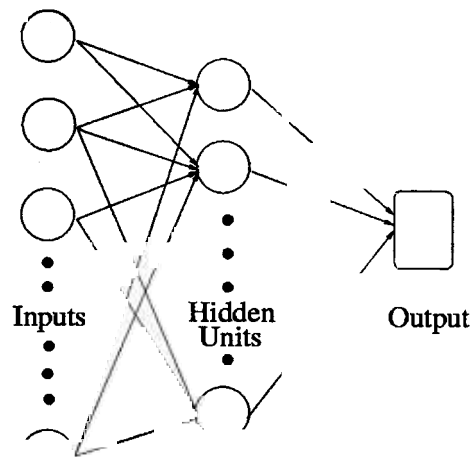


Fig. 1 The structure of the network

the Bayesian framework of our neural network analysis which makes possible the calculation of error bars whose magnitudes vary with the position in the input space, which define the range of useful applicability of the trained network. A visual impression of the spread of the data is shown in Fig. 2. Table 2 shows a selection of alloys which illustrate the range covered in the database.

Analysis

All the variables were normalised within a range of ± 0.5 as follows:

$$x_N = \frac{(x - x_{\min})}{(x_{\max} - x_{\min})} - 0.5 \quad (2)$$

where x_N is the normalised value of x , which has the minimum and maximum values given by x_{\min} and x_{\max} respectively. The normalisation is not necessary for the analysis but facilitates the subsequent comparison of the significance of each of the variables.

The database was randomised and then partitioned equally into test and training data sets. The latter was used to create a large variety of neural network models

Table 1 The variables used to develop the neural network model

Input element	Minimum	Maximum	Mean	Standard Deviation
Carbon/wt.%	2.3	4.05	3.56	0.181
Silicon/wt.%	2.0	3.58	2.56	0.244
Manganese/wt.%	0.01	1.52	0.33	0.229
Molybdenum*/wt.%	0.0	0.74	0.13	0.138
Nickel*/wt.%	0.0	4.83	0.37	0.598
Copper*/wt.%	0.0	2.00	0.29	0.348
Austenitising temperature/°C	800	1050	905	31.5
Austenitising time/min	15	480	79	38.3
Austempering temperature/°C	220	550	357	49.2
Austempering time/min	0.33	60 000	1419	8022
Austempering time $\log\{t_A/s\}$	1.96	6.556	3.60	0.886
Hardness/HV	194	693	392	93

* Molybdenum, nickel and copper were frequently not reported in publications since they were not deliberate additions, in which case their concentrations were set to zero

Table 2 A selection of alloys intended to illustrate the range covered in the database used to create the neural network model. The concentrations are in wt%

C	Si	Mn	Mo	Ni	Cu	Reference
4.05	2.1	0.19	0	1.14	0	[27]
3.67	2.45	0.20	0.30	0	0.78	[34]
3.3	2.5	0.21	0	1.6	1.6	[11]
3.16	3.09	0.17	0	0.8	0.03	[15]
3.52	2.64	0.67	0.25	0	0.25	[20]
3.05	2.17	0.85	0	1	0	[31]
3.75	2.29	0.37	0.32	1.41	0	[38]
3.74	2.63	1.14	0	0	1.34	[48]
3.51	2.81	0.25	0.13	0	0.39	[52]
3.3	2.95	1.52	0	0	0	[40]
3.52	2.6	0.2	0.2	0.41	0.73	[12]

whereas the test data set was used to see how the trained models generalised on unseen data.

Training involves the derivation of the weights by the minimisation of the regularised sum of squared errors σ_v . The complexity of the model is controlled by the number of hidden nodes, and the values of the regularisation constants,⁴ one associated with each input, one for biases and one for all weights connected to the output. The inferred noise level σ_v is expected to decrease as the number of hidden units increase (Fig. 3a). The number of hidden units is set by examining the performance of the model on unseen test data. The test set error tends to go through a minimum at an optimum complexity (Fig. 3b).

It is possible that a committee of models can make a more reliable prediction than an individual model.⁷⁴ The best models are ranked using the values of the test errors. Committees are then formed by combining the predictions of the best L models, where $L = 1, 2, \dots$; the size of the committee is therefore given by the value of L . A plot of the test error of the committee versus its size L gives a minimum which defines the optimum size of the committee as shown in Fig. 3c. The test error for a committee is calculated according to:

$$T_{\text{en}} = 0.5 \sum (\bar{Y}_n - t_n)^2 \quad \text{where} \quad \bar{Y}_n = \frac{1}{L} \sum y_n^{(l)} \quad (3)$$

The committee with ten models was found to have an optimum membership with the smallest test error (Fig. 3c). Once the optimum committee is chosen, it is retrained on the entire dataset without changing the complexity of each model, with the exception of the inevitable and relatively small adjustments to the weights.

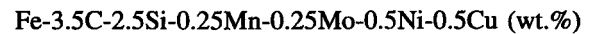
Fig. 4 shows normalised predicted values versus experimental values for the best model in the training and test datasets. The predictions made using the optimum committee of models are illustrated in Fig. 4c.

Fig. 5 illustrates the significance of each of the input variables, as perceived by the neural network in influencing the hardness. The magnitude of the significance is a measure of the extent to which a particular input explains

the variation in hardness. As expected, the logarithm of the austempering time features prominently. Fig. 6 shows that the effect of this variable in hardness is very non-linear.

Application of the model

The basic cast iron chosen to study the variations in hardness has the chemical composition



According to the literature⁷⁵⁻⁷⁸ this should have a low tendency to form intercellular carbides; at the same time, chemical segregation should not be excessive. The austemperability is expected to be around 32 mm in diameter, calculated using a relationship described by Lee and Voigt using $T_\gamma = 900^\circ\text{C}$.⁷⁹ The following predictions therefore indicate the influence of elements in the austempering process and its influence in hardness and microstructure.

The neural network can capture interactions between the inputs because the functions involved are nonlinear. The nature of these interactions is implicit in the values of the weights, but the weights are not always easy to interpret. For example, there may exist more than just pairwise interactions, in which case the problem becomes difficult to visualise from an examination of the weights. A better method is to actually use the network to make predictions and to see how these interactions depend on various combinations of inputs. Fig. 6 shows a contour plot which illustrate the interaction of two major variables in hardness predictions. First it shows that at low austempering time (t_A), the hardness increases as austempering temperature (T_A) increases. This is because the total amount of bainite that can form decreases as T_A increases, since the fraction of bainite is limited by the T_0 curve of the phase diagram. The T_0 curve is the locus of all points on the temperature versus carbon concentration plot where austenite and ferrite of the same chemical composition have identical free energies. The reaction is said to be incomplete, since it stops before the austenite has achieved its equilibrium composition^{80,81} given by the Ae_3 curve.

$$V_{\alpha_b} = \frac{x_{T_0} - \bar{x}}{x_{T_0} - x_{\alpha_b}} \quad (4)$$

where V_{α_b} is the volume fractions of bainitic ferrite at the point where the reaction stops, x_{T_0} is the carbon concentration given by the T_0 curve, \bar{x} is the average carbon concentration of the austenite prior to transformation, and x_{α_b} is the carbon concentration of the bainitic ferrite.

A second interesting point from the contour plot is that it shows that at low T_A , the hardness is maintained at a very high value even for large values of t_A . This is because even though V_{α_b} is large, the microstructure is very fine.⁸²

Unlike linear regression analysis, the range of applicability of a neural network model cannot be defined in terms of the range of the data used to create the model. This is because the network is non-linear so the inputs will

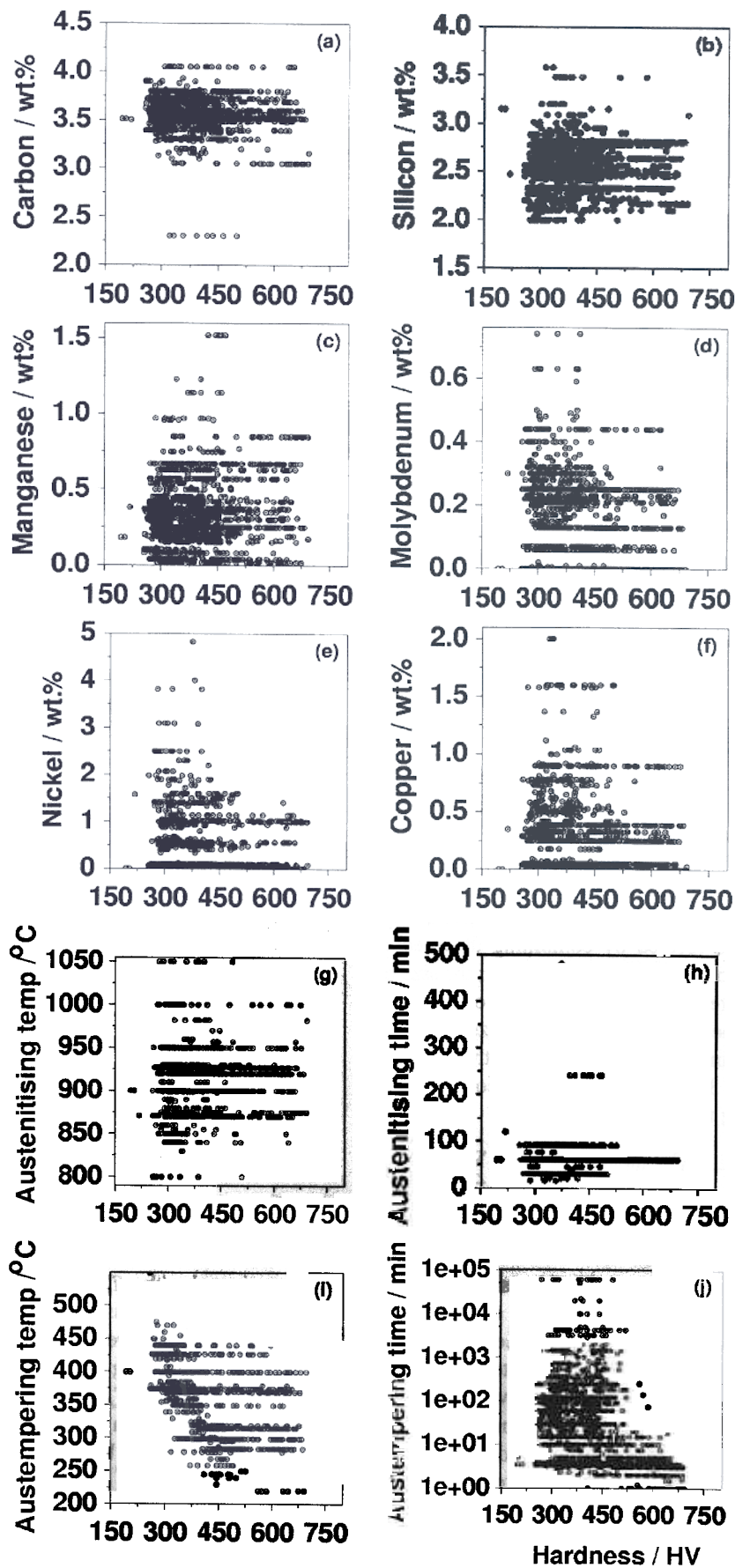


Fig. 2 The database values of each variable versus the hardness in HV

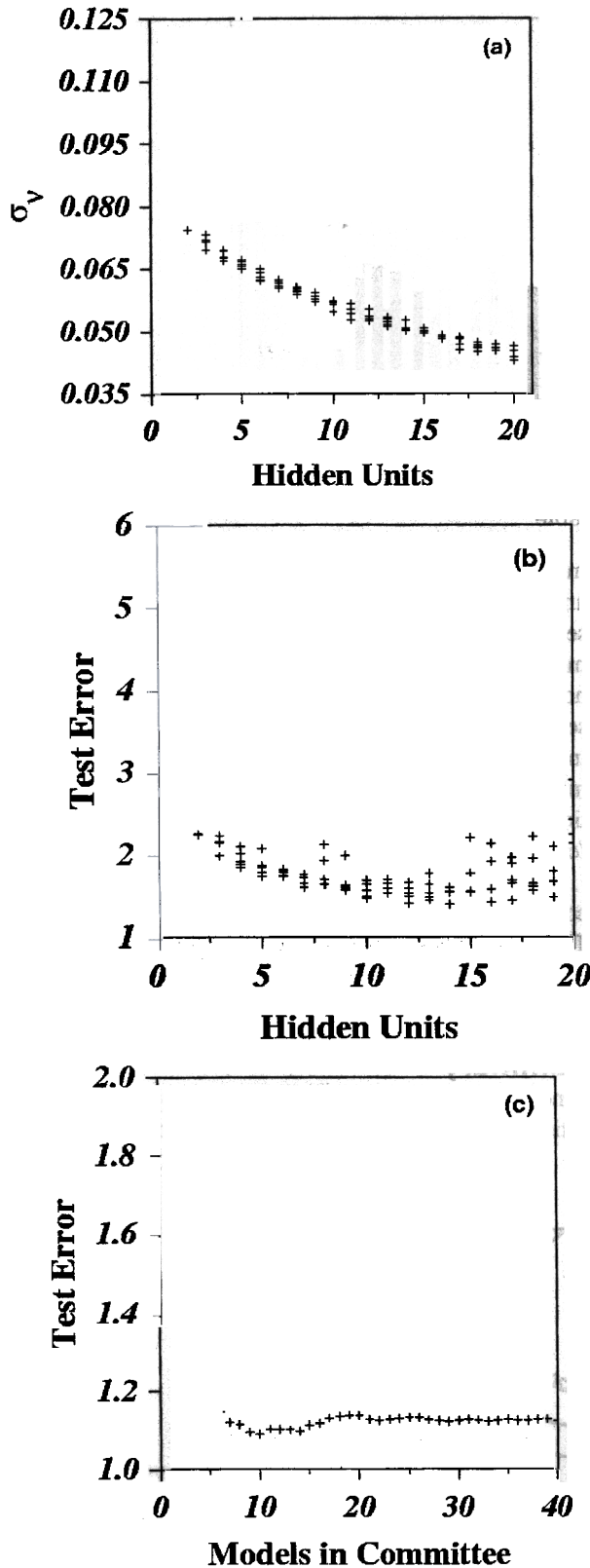


Fig. 3 (a) σ_v and (b) test error as a function of the number of hidden units; (c) the test error plotted as a function of the number of models in a committee of models

in general be expected to interact. It is the Bayesian framework of the present method which resolves this problem because it allows the calculation of error bars which define the range of useful applicability of the

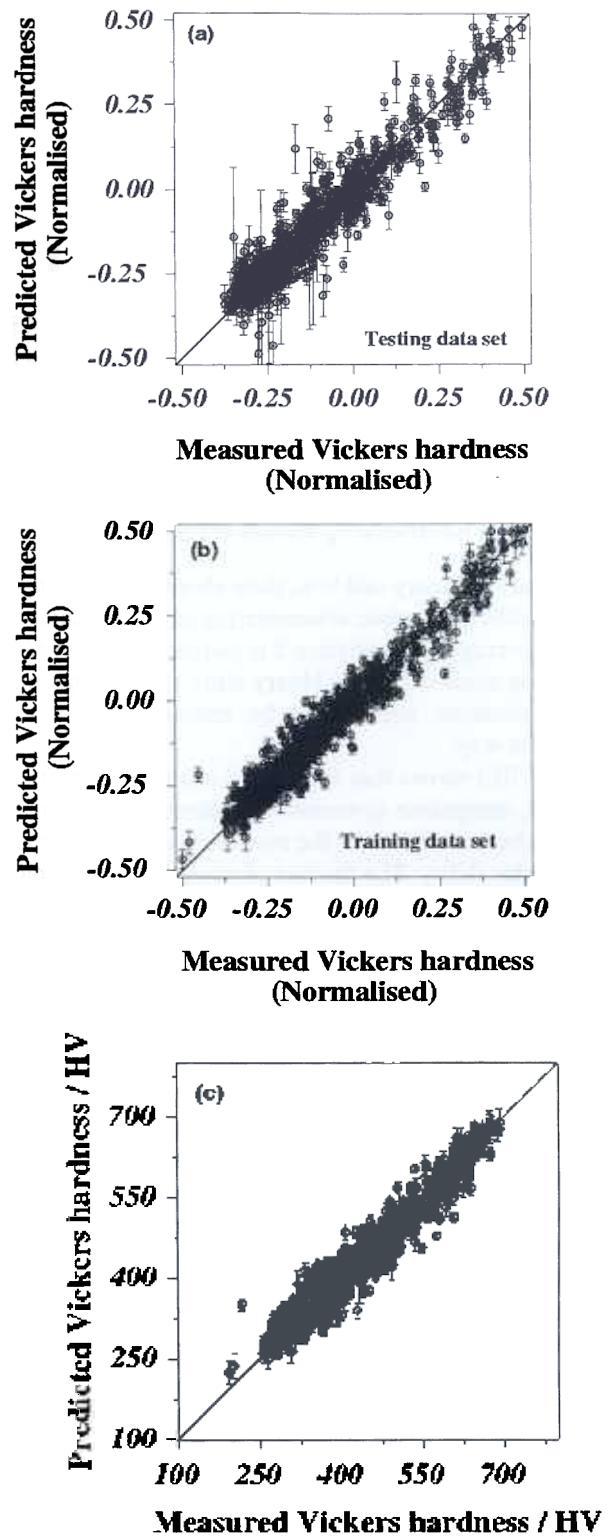
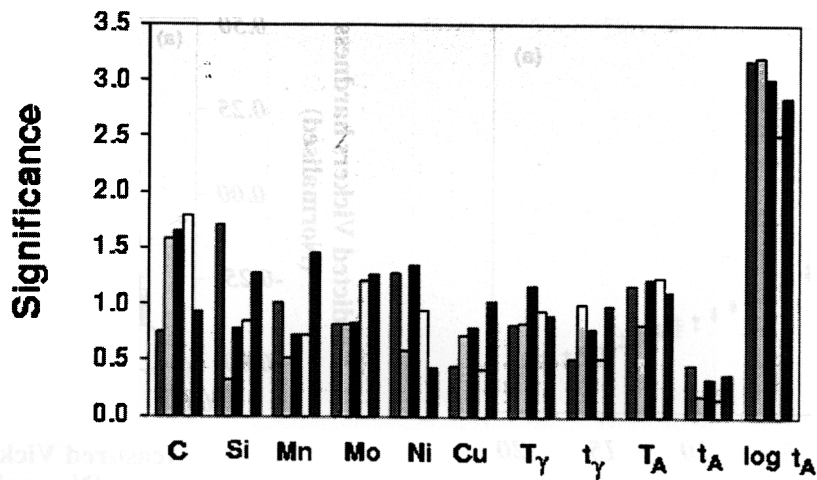


Fig. 4 Predictions made using the best model, selected as the one having the smallest test error. (a) Training data set. (b) Test data set. (c) Predictions made on the entire dataset using the optimum committee

trained network. The model can therefore be used in extrapolation given that it indicates appropriately large uncertainties when knowledge is sparse.

Fig. 7(a) shows that hardness increases slightly as the carbon concentration of the cast iron (\bar{x}) is increased from 3.1 to 3.6 wt.%. This is not clear since in an ideal pure



Model perceived significance of input parameters in the best five models from the committee trained on the hardness. σ_w values are presented for each variable

iron-carbon binary cast iron, there should be no change in the equilibrium carbon concentration of the austenite (x_γ) as the average concentration \bar{x} is increased. However, the cast iron studied is not a binary alloy but contains many other elements which may be interacting in a more complex way.

Fig. 7(b) shows that for a fixed austempering time of 60 min, manganese systematically increases the hardness. This is because it retards the transformation by increasing the hardenability. The fraction of martensite in the microstructure therefore increases causing a corresponding increase in hardness. There is of course, a small substitutional hardness effect as well. The effect of nickel illustrated in Fig. 7(d) can be similarly explained, although the uncertainty is greater because nickel is not usually added in large concentrations.

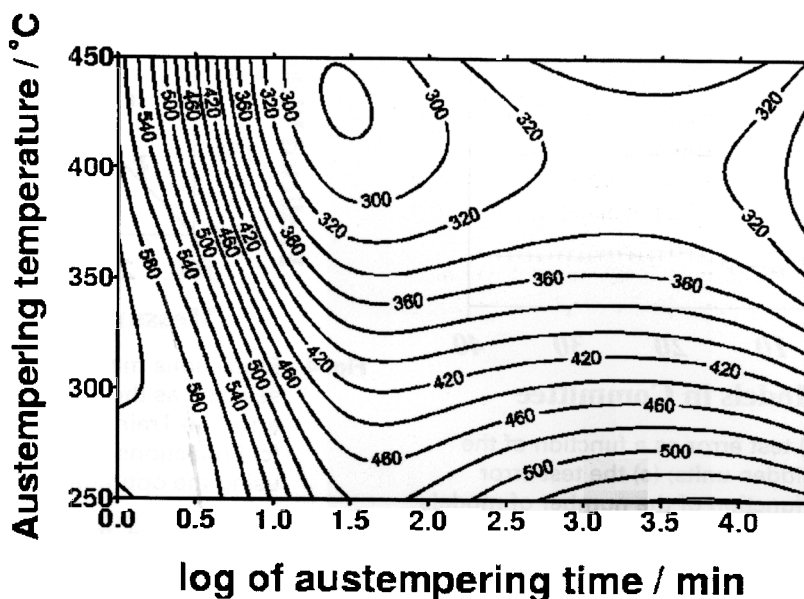
Fig. 7(c) shows an increase in hardness when molybdenum is increased from 0.0 to 0.1 wt.%, however, over this value there is a sharp decrease in hardness. Although

molybdenum does not have a marked influence on the amount of retained austenite,³ its influence in hardness seems to be significant. The decrease in hardness as molybdenum increase has been indicated to be due to non-uniform transformation response caused by negative segregation tendency of molybdenum.⁸³ Dorazil *et al.*⁸⁴ indicate that this behaviour is due to the segregation of molybdenum during solidification, resulting in the formation of stable intercellular carbides and also the local formation of martensite in the segregation regions.

Finally Fig. 8 shows some predictions which are compared with experimental data published by Kovacs.⁸⁵ This experimental data were not included in the input space of the present model.

Summary

A neural network model has been developed to enable the estimation of hardness in austempered ductile cast irons



Contour plot of hardness as a function of austempering time and temperature. Cast iron: Fe-3.5C-2.5Si-0.25Mn-0.25Mo-0.5Ni-0.5Cu wt.% austenitised at 900°C, for 60 min. The error bars associated with these predictions have been omitted for the sake of clarity

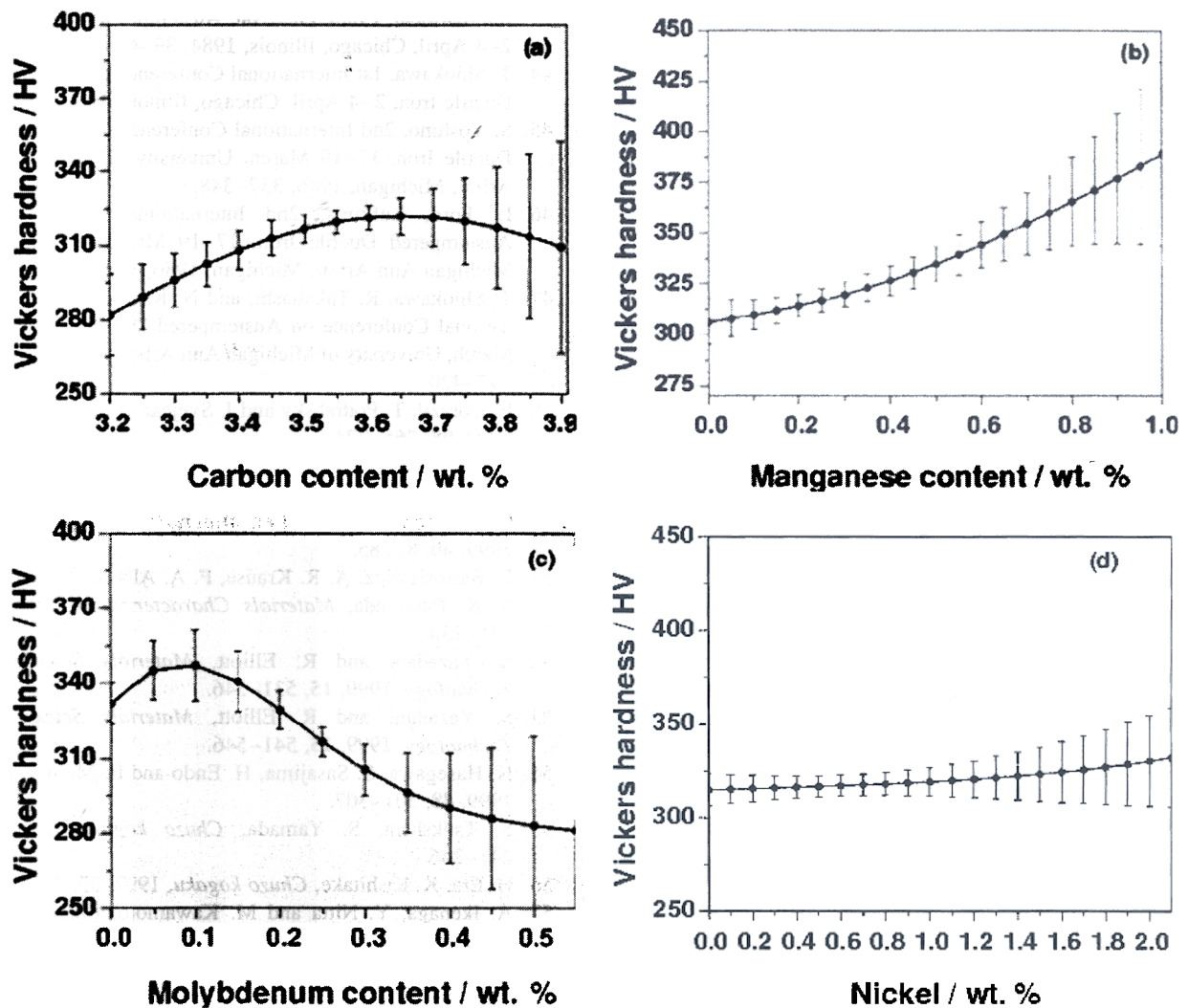


Fig. 7 Predictions of volume fraction of retained austenite in % as a function of chemical composition (Basic cast iron: Fe-3.5C-2.8Si-0.25Mn-0.25Mo-0.5Ni-0.5Cu wt.%). Austenitised at 900°C for 60 min, and austempered at 370°C for 60 min

as a function of their chemical composition (C, Mn, Si, Ni, Mo, Cu), the austenitisation and austempering parameters. The model successfully reproduces experimental trends observed by other researchers. It can be exploited in two ways, first in the design of cast irons and their heat treatments, but also to identify whether experiments are needed in the future. If the model prediction is associated with a large uncertainty then an experiment can be considered to be novel and useful. The model can also be used to find more complex relationships between variables.

The computer program associated with this work can be obtained freely from the *Materials Algorithms Project Library* on: <http://www.msm.cam.ac.uk/map/mapmain.html>

Acknowledgements

I am grateful to Professor D. J. Fray for the provision of laboratory facilities at the University of Cambridge. I am indebted to Prof. H. K. D. H. Bhadeshia for helpful comments on this paper. I would like to thank the

National Council of Science and Technology of Mexico (CONACYT) for a scholarship.

References

1. M. A. Yescas, Thesis, University of Cambridge, 2001.
2. D. J. Moore, T. N. Rouns and K. B. Rundman, *AFS Trans.*, 1986, **9**, 255–264.
3. M. A. Yescas, H. K. D. H. Bhadeshia and D. J. MacKay, *Materials Science and Engineering A*, 2001, **311**, 162–173.
4. D. J. C. MacKay, in: H. Cerjack, (Ed.), *Mathematical Modelling of Weld Phenomena 3* Graz, Austria, 1997, p. 359.
5. H. Fuki and H. K. D. H. Bhadeshia, *ISIJ Int.*, 1999, **39**, 965–979.
6. R. C. Eberhart and R. W. Dobbins, *Neural networks PC Tools*. Academic Press, Inc., California 1990.
7. D. J. C. MacKay, *Neural Computation*, 1992, **4**, 415.
8. D. J. C. MacKay, *Neural Computation*, 1992, **4**, 448.
9. S. E. Stenfors, J. Storesun and R. Sandstrom, 2nd International Conference on Austempered Ductile Iron, 17–19 March, University of Michigan Ann Arbor, Michigan, 1986, 227–236.

10. M. Aoyama and T. Kobayashi, *Cast Metals*, 1990, **3**, 122–128.
11. M. Grech and J. M. Young, *Cast Metals*, 1988, **1**, 98–103.
12. J. M. Prado, A. Pujol, J. Cullerell and J. Tartera, *Materials Science and Technology*, 1995, **11**, 294–298.
13. G. J. Cox, *The British Foundryman*, 1986, June, 215–219.
14. N. Darawish and R. Elliott, *Materials Science and Technology*, 1993, **9**, 572–585.
15. W. J. Dubensky, K. B. Rundman, *AFS Trans.*, 1985, **94**, 389–394.
16. R. C. Voigt, *AFS Transactions*, 1983, **92**, 253–262.
17. E. Dorazil, T. Podrabsky and J. Svejcar, *AFS Transactions*, 1990, **98**, 765–774.
18. I. Singh and S. K. Putatunda, *Trans. Indian Inst. Met.*, 1994, **47**, 317–325.
19. T. N. Rouns, K. B. Rundman and D. M. Moore, *AFS Transactions*, 1984, **92**, 815–840.
20. H. Bayati and R. Elliott, *Materials Science and Technology*, 1995, **11**, 118–129.
21. J. M. Velez, A. Garboggini and A. P. Tschiptchin, *Materials Science and Technology*, 1996, **12**, 329–337.
22. M. Grech and J. M. Young, *AFS Transactions*, 1990, **98**, 345–353.
23. R. Viau, M. Gagne and R. Thibau, *AFS Transactions*, 1987, **95**, 171–178.
24. M. N. Ahmadabadi, S. Nategh and P. Davami, *Cast Metals*, 1992, **4**, 188–194.
25. C. K. Lin and J. Y. Wei, *Materials Transactions JIM*, 1997, **38**, 682–691.
26. K. L. Hayrynen, G. P. Faubert, D. J. Moore and K. B. Rundman, *AFS Transactions*, 1989, **97**, 747–756.
27. S. Korichi and R. Priestner, *Materials Science and Technology*, 1995, **11**, 901–907.
28. R. Kazerooni, A. Nazarboland and R. Elliott, *Materials Science and Technology*, 1997, **13**, 1007–1015.
29. A. S. Hamid and R. Elliott, *Materials Science and Technology*, 1996, **12**, 679–690.
30. M. N. Ahmadabadi, *Cast Metals*, 1992, **5**, 62–72.
31. D. A. Harris, B. Tech and R. J. Maitland, *Iron and Steel*, 1970, 53–60.
32. L. Sidjanin, R. E. Smallman and J. M. Young, *Acta Metall. Mater.*, 1994, **42**, 3149–3156.
33. H. Bayati and R. Elliott and G. W. Lorimer, *Materials Science and Technology*, 1995, **11**, 776–786.
34. W. S. Zhou, Q. D. Zhou and S. K. Meng, *Cast Metals*, 1993, **6**, 69–75.
35. B. Y. Lin, E. T. Chen and T. S. Lei, *Scripta Metallurgica et Materialia*, 1995, **32**, 1363–1367.
36. T. S. Shih and Z. C. Yang, *Int. J. Cast. Met. Res.*, 1998, **10**, 335–344.
37. I. Schmid and A. Schuchert, *Z. Metallkde*, 1987, **78**, 871–875.
38. P. Shanmugam, P. Prasad, K. U. Rajendra and N. Venkataraman, *Journal of Materials Science*, 1994, **29**, 4933–4940.
39. S. K. Putatunda and P. K. Gadicherla, *Materials Science and Engineering*, 1999, **A286**, 15–31.
40. A. Owhadi, J. Hedjazi and P. Davami, *Materials Science and Technology*, 1998, **14**, 245–250.
41. J. S. Schissler, J. Chabaut, C. Bak and D. Gouvenel, 2nd International Conference on Austempered Ductile Iron, University of Michigan, 1986, 149–155.
42. M. M. Shea, E. F. Ryntz, *AFS Transactions*, 1986, **94**, 683–688.
43. L. Robinson, W. M. Spear and G. W. Tuffnell, 1st International Conference on Austempered Ductile Iron, 2–4 April, Chicago, Illinois, 1984, 39–43.
44. T. Shiokawa, 1st International Conference on Austempered Ductile Iron, 2–4 April, Chicago, Illinois, 1984, 107–115.
45. S. Yoshino, 2nd International Conference on Austempered Ductile Iron, 17–19 March, University of Michigan Ann Arbor, Michigan, 1986, 337–348.
46. L. Ford, Lufkin's, 2nd International Conference on Austempered Ductile Iron, 17–19 March, University of Michigan Ann Arbor, Michigan, 1986, 367–372.
47. T. Shiokawa, R. Takahashi, and N. Kawamoto, 2nd International Conference on Austempered Ductile Iron, 17–19 March, University of Michigan Ann Arbor, Michigan, 1986, 397–420.
48. E. Dorazil, T. Podrabsky and J. Svejcar, *AFS Transactions*, 1990, **98**, 765–774.
49. S. Yazadani and R. Elliott, *Materials Science and Technology*, 1999, **15**, 885–894.
50. C. T. Chen and T. S. Lei, *Materials Transactions, JIM*, 1999, **40**, 82–85.
51. L. Bartosiewicz, A. R. Krause, F. A. Alberts, I. Singh and S. K. Putatunda, *Materials Characterization*, 1993, **30**, 221–234.
52. S. Yazadani and R. Elliott, *Materials Science and Technology*, 1999, **15**, 531–546.
53. S. Yazadani and R. Elliott, *Materials Science and Technology*, 1999, **15**, 541–546.
54. N. Hasegawa, S. Sasajima, H. Endo and E. Marui, *Zairyo*, 1999, **48**, 301–307.
55. S. Tsukshsra, S. Yamada, *Chuzo kogaku*, 1998, **70**, 241–246.
56. H. Era, K. Kishitake, *Chuzo kogaku*, 1997, **69**, 911–916.
57. A. Ikenaga, Y. Nitta and M. Kawamoto, *Chuzo kogaku*, 1996, **68**, 585–591.
58. K. Nagai, H. Era and K. Kishitake, *Imono*, 1994, **66**, 827–832.
59. K. Shimizu, T. Naguchi, *Imono*, 1994, **66**, 489–494.
60. T. Takahashi, S. Tada and T. Abe, *Imono*, 1993, **65**, 615–620.
61. K. Hori and T. Kobayashi, *Imono*, 1993, **65**, 777–782.
62. H. Kage and Y. Tanaka, *Imono*, 1993, **65**, 382–387.
63. T. Kovayashi, K. Hori and S. Yamada, *Imono*, 1993, **65**, 197–203.
64. Y. Tanaka, A. Shimizu and H. Yokouchi, *Imono*, 1993, **65**, 93–98.
65. H. Sunada, *Zairyo*, 1991, **40**, 669–674.
66. T. Fujita, K. Ogi, T. Fukui and M. Suenaga, *Imono*, 1991, **63**, 775–780.
67. H. Yamamoto, Y. Ji, T. Kobayashi, *Imono (Journal of the Japan Foundrymen's Society)*, 1990, **62**, 810–815.
68. T. Yoshida, K. Komatsu and S. Okada, *Imono*, 1993, **65**, 221–226.
69. H. P. Feng, S. C. Lee, C. H. Hsu and J. M. Ho, *Materials Chemistry and Physics*, 1999, **59**, 154–161.
70. M. N. Ahmadabadi, H. M. Ghasemi and M. Osia, *Wear*, 1999, **231**, 293–300.
71. C. K. Lin and W. J. Lee, *International Journal of Fatigue*, 1997, **20**, 301–307.
72. D. C. Wen and T. S. Lei, *ISIJ International*, 1999, **39**, 493–500.
73. R. C. Dommarco, P. C. Bastias, H. A. Dall'O, G. T. Hahn and C. A. Rubin, *Wear*, 1998, **221**, 69–74.
74. D. J. C. MacKay, *Neural Computation*, 1992, **4**, 698.
75. E. Dorazil, *Ellis Horwood Series in Metals and Associated Materials*, Series Editor: E. G. West, *Obe*, 1991, 43–47.

76. T. N. Rouns and K. B. Rundman, *AFS Trans.*, 1987, **95**, 851–874.
77. Y. Ueda and M. Takita, 2nd International Conference on Austempered Ductile Iron, University of Michigan, 1986, 141–147.
78. R. C. Voigt, *Cast. Met.*, 1989, **2**, 72–93.
79. Y. H. Lee and R. C. Voigt, *AFS Trans.*, 1989, **97**, 915–938.
80. H. K. D. H. Bhadeshia and D. V. Edmonds, *Acta Metall.*, 1980, **28**, 1103–1114.
81. H. K. D. H. Bhadeshia and D. V. Edmonds, *Metall. Trans.*, 1979, **10A**, 895–907.
82. F. G. Caballero, H. K. D. H. Bhadeshia, K. J. A. Mawella, D. G. Jones and P. Brown, *Materials Science and Technology*, 2001, **17**, 512–516.
83. R. C. Voigt and C. R. Loper, *Journal of Heat Treating*, 1984, **3**, 291–309.
84. E. Dorazil, B. Barta, E. Munsterova, L. Stransky and A. Huvar, *AFS International Cast Metals Journal*, 1982, 52–62.
85. B. V. Kovacs, J. R. Keough and D. M. Pramstaller, Austempered Ductile Iron (ADI) Process Development, Gas Research Institute Report GRI-89/0017, Chicago, Illinois, 1989.

(Received 15 September 2001, accepted 1 April 2002)